Effect of an Insoluble Surfactant on Capillary Oscillations of Bubbles in Water: Observation of a Maximum in the Damping

T. J. Asaki,* D. B. Thiessen, and P. L. Marston
Department of Physics, Washington State University, Pullman, Washington 99164-2814
(Received 19 July 1995)

The excess damping of capillary waves caused by a surfactant monolayer is demonstrated to be present as well for the quadrupole shape mode of an isolated acoustically trapped bubble in water. To facilitate measurements of damping as a function of surface concentration, a method was developed for depositing a known amount of insoluble surfactant (stearic acid) on the surface of the bubble. As the bubble dissolves, the stearic acid concentration increases, and the excess damping has a pronounced local maximum near 0.26 nm^2 per molecule specific area in agreement with capillary wave data for a flat surface. The method of depositing insoluble surfactant should be applicable to the characterization of other surface-limited processes in isolated bubbles.

PACS numbers: 43.25.+y

Naturally produced or man-made bubbles are central to a variety of sonochemical, transport, and sensing processes, and surfactant-related studies [1–3]. Surfactant coatings on bubbles affect their physical and temporal stability, and contribute to bubble-mediated transport [2–5]. Here we measure the prominent effects of an insoluble surfactant on shape oscillations bubble tensiometry [1,5,6] which involve primarily surface dilatational responses to pressure changes within a bubble at the tip of a capillary. Our method of depositing the surfactant may have application to other acoustically trapped bubbles such as in single-bubble sonoluminescence [7]. Capillary oscillations of the bubble are excited using the method of modulated ultrasonic radiation pressure [8] developed for noncontact drop-dynamic studies [9,10] and recent studies of bubbles in pure water and seawater [11]. The properties of the quadrupole mode were measured as a function of the surface coverage of stearic acid. The normalized damping has a local maximum at a stearic acid coverage similar to that for the damping of capillary waves on flat water surfaces [12,13]. While trends in mode frequency and damping are generally consistent with predictions, and unexpected increase in frequency is observed at high coverage.

The surface of clean water is generally characterized by the surface tension alone, however, when the surface is covered with a monolayer of surfactant, it also exhibits surface elasticity and viscosity which are known to greatly affect the damping of capillary waves. These surface properties are dependent on the concentration of surfactant. Some of the numerous studies of surfactant-enhanced damping of capillary waves [12–18] were motivated in part by the general calming effect of oil films on the sea surface. The geometry of a bubble, in the present work, places certain constraints on capillary waves which has an effect on the bubble dynamics [11,19]. Appreciable damping arises from the liquid and gas viscosities, as well as from processes modeled as surface viscosity and elasticity.

In our experiment, an air bubble in water is trapped in a 23 kHz ultrasonic standing wave and driven into axisymmetric shape oscillation by modulation of the standing wave amplitude [8]. The quadrupole mode involves oscillation between oblate and prolate shapes. The acoustical and optical components of the apparatus are described in Ref. [11]. They include a levitation chamber made of PMMA which has an ultrasonic transducer mounted in the bottom (Fig. 1). The ultrasonic transducer consists of a cylindrical piezoelectric elements with a glass plate cemented to the top. The expanded beam of an intensity-stabilized He-Ne laser is directed through the cell from the bottom in such a way that the bubble is centered in the beam. On top of the cell the beam

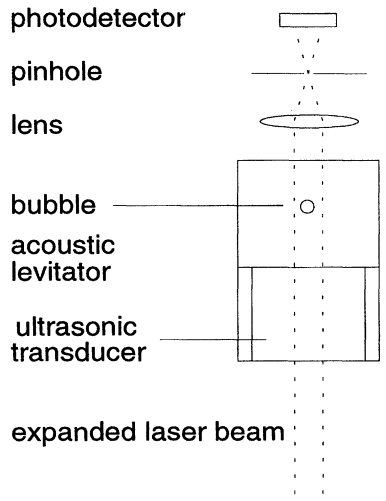

FIG. 1. Schematic representation of the experimental setup. The photodetector monitors the freely decaying quadrupole oscillations of the bubble. The bubble radii, typically in the range 0.7–0.5 mm, are much smaller than the dimensions of the acoustic levitator which contains 570 mℓ of water. The levitator is used to trap the bubble and to excite shape oscillations.

 0031-9007/95/75(14)/2686(4)$06.00

is focused onto a photodetector. Slight changes in the cross sectional area of the bubble are detected as intensity changes by the photodetector. When a bubble is undergoing small amplitude quadrupole shape oscillations, the cross section changes sinusoidally. The modulation frequency is tuned to give the maximum response of the sinusoidal photodetector signal corresponding to the natural resonance of the bubble shape mode. The shape oscillations cause variations in the local radius that are less than 10% of the mean radius. The modulation of the ultrasonic standing wave is then terminated and the decay signal digitally recorded to give frequency and damping measurements. The records are fit by the formula $A(t) = A_0 \exp(-\beta t) \sin(2\pi\nu t + \phi)$, where ν and β are the free-decay frequency and damping.

Stearic acid monolayers were spread on the bubble surface using HPLC grade denatured ethanol (5% isopropanol) as the spreading solvent. Stearic acid [$CH_3(CH_2)_{16}COOH$] was chosen for investigation because it is insoluble in water, and there is a negligible effect of the subphase pH on monolayer properties [20]. The host water was prepared as follows: Water was deionized and then distilled directly into teflon storage bottles. The PMMA sample chamber was rinsed with copious amounts of distilled water prior to filling for each bubble studied. In the absence of surfactant, for the bubble size range studied, the measured β and ν were in agreement with values predicted for a spherical air bubble in pure water as previously described [11]. (The frequency ν differs from the predicted value by about 1%, which is similar to the deviation of the bubble's aspect ratio from unity due to the static component of radiation stress [21]). Placing a monolayer of surfactant on the surface of a small bubble requires precise delivery of a small volume of dilute surfactant solution. For this purpose we have used a Hamilton microliter syringe (model 7001) which has a capacity of 1 $\mu\ell$. The syringe was mounted on a translation stage so that the needle tip could be precisely positioned on the bubble surface. The needle tip must be in contact with the bubble surface during the entire time that the solution is being injected. Injection of the surfactant solution had to proceed very slowly because of violent bubble motion arising from Marangoni motion of the interface. Following surfactant injection on a levitated bubble, the needle tip must be withdrawn rapidly so that the bubble surface detaches without dislodging the bubble from the potential well of the acoustic radiation pressure. The method of surfactant delivery described above was tested, using surface tension measurements of pendant bubbles which were close to the same size as those studied in the levitator. Surface tension and surface area measurements of the pendant bubble were made as the bubble dissolved, using digital image analysis. Data obtained in this way were compared to literature data [20] to confirm that the full amount of surfactant has indeed been delivered to the surface.

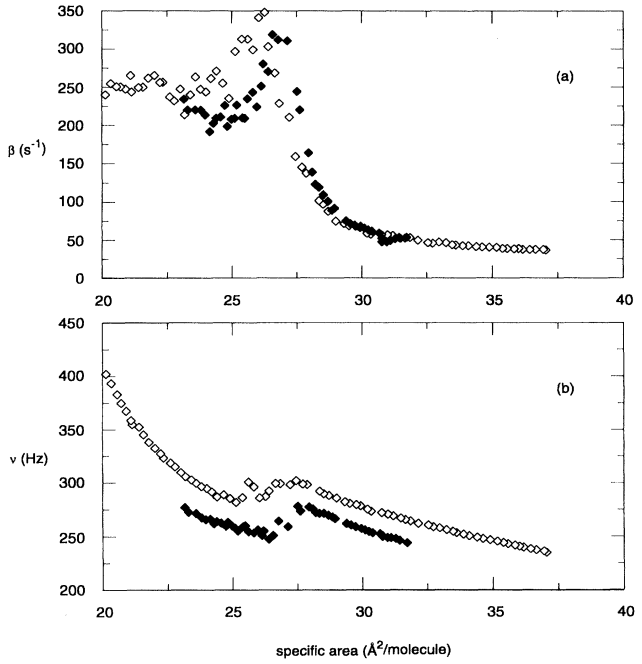

FIG. 2. Measurements of (a) damping and (b) frequency of the quadrupole mode of two bubbles shown as a function of stearic acid surface concentration. Differences in frequency and damping are expected since the bubbles do not have the same radius for a given surface concentration; the radius at maximum damping is 668 and 625 μm for the closed and open symbols, respectively, and the minimum recorded radii are 622 and 548 μm.

Frequency and damping measurements for free decay of bubble oscillations were made as a function of surface coverage. Bubbles of approximately 2 mm diameter were injected with 0.85–1.0 $\mu\ell$ of $3.7 \times 10^{-5} M$ stearic acid solution to give initial surface coverages of 60 Å^2/molecule. Surface coverage increases with time, since the bubble shrinks as the air inside slowly dissolves into the surrounding water. Monolayer compression rates ranged from 0.09–0.18 Å^2/molecule min for different bubbles. Once the diameter was smaller than 1.5 mm, mode decay traces were recorded. The bubble surface area was measured concurrently from digital images.

Figure 2 gives frequency and damping measurements as a function of surface coverage. These are normalized in Fig. 3 with respect to the corresponding values for a clean surface bubble calculated as in Ref. [11] for each radius. Figure 4 shows theoretical results using the model of Miller and Scriven [Eq. (23) of Ref. [19]]. Figures 3 and 4 cannot be compared, directly, since the model results are computed as a function of dilatational surface elasticity. Dilatational elasticity is known to increase with increasing surface coverage (decreasing specific area), although the precise relationship is unknown for this system. Also, the theoretical results assume constant

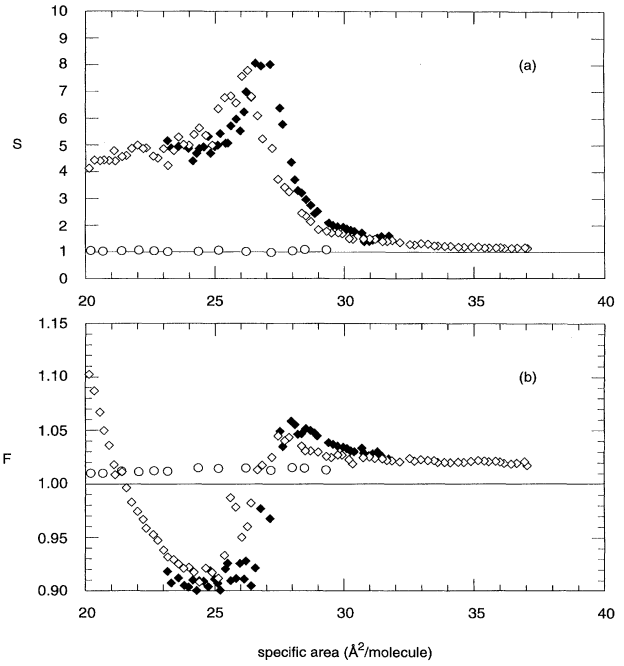

FIG. 3. The diamond symbols show the (a) damping and (b) frequency from Fig. 2 normalized by the theoretical value for a bubble with a clean surface in pure water, having a radius corresponding to that of each measurement. By suppressing the drift in damping and frequency associated with the drift in bubble size, the normalized data more clearly show the effects of increasing the surface coverage. The open circles are for a control run in which 1 $\mu\ell$ of ethanol was injected on the bubble surface instead of stearic acid solution. (The horizontal axis in this case gives the concentration that would have been present had 1 $\mu\ell$ of $3.7 \times 10^{-5} M$ stearic acid solution been injected.) The frequency and damping are unaffected by the ethanol.

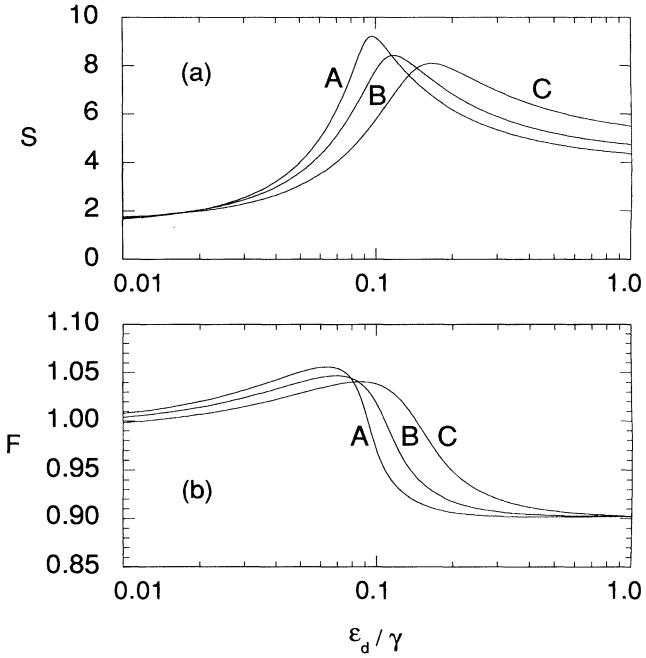

FIG. 4. Model results for (a) the normalized damping S and (b) the normalized frequency F for free decay of the quadrupole mode of a bubble as a function of normalized surface dilatational elasticity. Unlike Figs. 2 and 3, the right hand side corresponds to high surface coverage. Calculations are for a bubble of radius 668 μm, surface tension $\gamma = 72.3$ dyn/cm, surface shear elasticity $\varepsilon_s = 0$, and normalized surface dilatational viscosity $\hat{\eta}_d = 0.005$, where $\hat{\eta}_d = \omega \eta_d / \gamma$. The curves A, B, and C correspond to normalized surface shear viscosities of $\hat{\eta}_s = 0.025$, 0.05, and 0.1, respectively. Calculations (not shown) indicated that for $\varepsilon_d / \gamma \gtrsim 0.3$, both S and F depend very weakly on $\hat{\eta}_d$. This facilitates comparison with Fig. 3 in the region where the specific area is less than 25 Å^2/molecule, and S and F are close to 5 and 0.9, respectively. The observed maxima in S and associated local maxima in F in Fig. 3 are also similar in magnitude to the model, as are the limiting values at high specific areas.

surface properties (besides elasticity) and constant bubble radius, which is not realized in the experiments. The magnitude of the normalized frequency and damping can be compared to theory in various regions noted in the caption. The damping peak occurs at a low value of elasticity, which for stearic acid means that the surface tension is nearly the same as for pure water. Figure 4 is evaluated for a bubble with the surface tension of pure water and with the same radius at which the experimental damping peak was seen. The two components of surface viscosity (shear and dilatational) were adjusted so that the model would give both the frequency and damping peak heights comparable to the measured peak heights. By fitting only the damping and frequency peaks, however, the model is seen to properly predict the frequency and damping at higher surface coverages (higher elasticity). At the highest surface coverage studied, an unexpected increase in the frequency is observed.

It is a appropriate to compare the location of the damping maximum with the location found by other in traditional capillary wave experiments, utilizing stearic acid monolayers on a 2.0 pH solution of hydrochloric acid, since [20] stearic acid monolayers are insensitive to pH. Maxima in the damping near 24 Å^2 per molecule are reported [12,13] for 180 and 520 Hz. Ignoring possible weak curvature and frequency effects, the value observed here of 26 Å^2 per molecule suggests that the systematic uncertainty associated with the monolayer application technique is a small fraction of the total coverage.

The method of depositing a known concentration of insoluble surfactant on an acoustically trapped or levitated bubble offers the possibility of affecting the rate of gas diffusion to or from a radially pulsating bubble. Processes strongly affected by diffusion across the surface of a pulsating bubble include single-bubble sonoluminescence [7,22] and bubble growth through rectified diffusion [23].

This research was supported by the U.S. Office of Naval Research.

*Present address: Group MST-10, Los Alamos National Laboratory, Los Alamos, NM 87544.

[1] D. O. Johnson and K. J. Stebe, J. Colloid Interface Sci. **168**, 21 (1994).
[2] T. G. Leighton, *The Acoustic Bubble* (Academic Press, London, 1994).
[3] *Climate and Health Implications of Bubble-Mediated Sea-Air Exchange* edited by E. C. Monahan and M. A. Van Patten (Connecticut Sea Grant Program, 1989).
[4] B. D. Johnson and R. C. Cooke, Science **213**, 209 (1981).
[5] D. A. Edwards, H. Brenner, and D. T. Wasan, *Interfacial Transport Processes and Rheology* (Butterworth-Heinemann, Boston, 1991).
[6] S. B. Hall *et al.,* J. Appl. Phys. **75**, 468 (1993).
[7] L. A. Crum, Phys. Today **47**, No. 9, 22 (1994); S. J. Putterman, Sci. Am. **272**, No. 2, 46 (1995).
[8] P. L. Marston, , and , J. Accoust. Soc. Sm. **67**, 15 (1980).
[9] E. H. Trinh, A. Zwern, and T. G. Wang, J. Fluid Mech. **115**, 453 (1982).
[10] H. Lu and R. E. Apfel, J. Fluid Mech. **222**, 351 (1991).
[11] T. J. Asaki and P. L. Marston, J. Fluid Mech. **300**, 149 (1995).
[12] B. A. Noskov, Colloid J. **50**, 1035 (1988).
[13] B. A. Noskov and T. U. Zubkova, J. Colloid Interface Sci. **170**, 1 (1995).
[14] E. H. Lucassen-Reynders and J. Lucassen, Adv. Colloid Interface Sci. **2**, 347 (1969).
[15] E. J. Bock and J. A. Mann Jr., J. Colloid Interface Sci. **129**, 501 (1989).
[16] W. Alpers and H. Huhnerfuss, J. Geophys. Res. **94**, 6251 (1989).
[17] J. C. Scott, Nature (London) **340**, 601 (1989).
[18] K. Sakai and K. Takagi, Langmuir **10**, 257 (1994).
[19] C. A. Miller and L. E. Scriven, J. Fluid Mech. **32**, 417 (1968).
[20] G. L. Gaines, Jr., *Insoluble Monolayers at Liquid-Gas Interfaces* (Wiley, New York, 1966), pp. 219–226.
[21] T. J. Asaki and P. L. Marston, J. Acoust. Soc. Am. **97**, 2138 (1995).
[22] B. P. Barber *et al.,* Phys. Rev. Lett. **72**, 1380 (1994).
[23] M. M. Fyrillas and A. J. Szeri, J. Fluid Mech. **289**, 295 (1995).